Computational Study of the Mechanism of Dehydrogenative Borylation of Terminal Alkynes by SiNN Iridium Complexes

Jia Zhou[1], Chun-I Lee[2], and Oleg V. Ozerov[2]**

[1] MIIT Key Laboratory of Critical Materials Technology for New Energy Conversion and Storage, School of Chemistry and Chemical Engineering, Harbin Institute of Technology, Harbin 150001, China

[2]Department of Chemistry, Texas A&M University, College Station, TX 77842, USA

jiajoe@gmail.com

ozerov@chem.tamu.edu

ABSTRACT. This paper presents a comprehensive study of the mechanism of dehydrogenative borylation of terminal alkynes (DHBTA) by Ir complexes of the SiNN pincer ligands. The study uses phenylacetylene as the prototypical alkyne and pinacolborane (HBpin) as the boron source. The original report (*J. Am. Chem. Soc*. **2013**, *135*, 3560) on this reactivity proposed, without any substantial evidence, a mechanism similar to that usually ascribed to Ir catalysts for aromatic C-H borylation. However, this work has uncovered a completely different mechanistic picture. Three interlinked mechanistic pathways have been identified. The free energy barriers lie in the ca. 16-22 kcal/mol range, qualitatively compatible with the experimentally observed turnover rate on the order of 0.1 s^{-1}. The key element in all three pathways is the facile migration of the Bpin group between Ir and the N(amido) of the ancillary SiNN ligand. In particular, migration of Bpin onto N(amido) opens up the Ir center electronically and coordinatively for a more facile C-H oxidative addition step. The Si-H moiety of the SiNN ligand is also non-innocent as its nature of the interaction with the Ir center fluctuates between complete oxidative addition of the SiH bond and a σ-complex interaction. In addition to the identification of three different catalytic cycles with plausible overall barriers, many transition states within each cycle possess similar energies. Thus, in this system it is not possible to identify a dominant high-lying transition state with confidence, especially considering that the relative energies of the closely spaced states is likely to vary depending on the nature of the alkyne substrate and on the different reagent concentrations throughout the course of the reaction. Nonetheless, it is the presence of the multiple possible low-energy pathways that must be responsible for the effective catalysis of DHBTA by the (SiNN)Ir system.

KEYWORDS: C-H borylation, pincer ligands, iridium, DFT calculations, mechanism, alkyne, DHBTA, alkynylboronate.

Introduction

Synthesis of organoboronic esters or organoboronic acids by catalytic borylation of C-H bonds (Scheme 1) has developed into a burgeoning field over the last two decades.[1-6] Organoboronic acids and their derivatives are versatile and easily handled synthetic building blocks, whose use in a large variety of carbon-carbon and carbon-heteroatom making reactions is well documented.[7] Catalysts based on iridium and supported by neutral bidentate ligands such as bis(phosphines), bipyridines, and phenanthrolines have emerged as arguably the most prolific catalytic system, in particular for the borylation of aromatic C-H bonds.[8] The mechanism of the catalysis in these systems is believed to proceed via boryl-substituted trivalent iridium intermediates.[3-6] This insight has allowed the development of new designs aimed at further improving activity and selectivity.[9-11] Interestingly, our own recent work on the catalysis of aromatic C-H borylation with pincer complexes of Ir suggested that high activity with Ir can arise via mechanisms that do not rely on trivalent Ir boryl intermediates.[12] Other recent work reported on the C-H borylation mediated by Co,[13-16] Pt,[17] Fe,[18] heterobimetallic Fe/Cu catalysts,[19] as well as metal-free borylation.[20] Among the various types of C-H bonds, the borylation of aromatic C(sp^2)-H bonds has arguably seen the most attention and success, however, borylation of other types of C(sp^2)-H bonds and of C(sp^3)-H bonds has also been accomplished.[21-29] On the other hand, catalytic dehydrogenative borylation of terminal alkynes (DHBTA) involving the C(sp)-H bonds remained unknown until 2013. Alkynylboronates, the products of DHBTA, have been used in C-C coupling,[30] but their greater synthetic potential lies in the various reactions possible at the triple bond, delivering more complex organic molecules with preserved organoboronate functionalities suitable for further elaboration.[31-34] In 2013, our group reported DHBTA utilizing an Ir catalyst supported by a new SiNN-type pincer ligand that contains a hydrosilane, an amido and a quinoline set of donors (**1**, Scheme 2).[35] Turnover numbers on the order of 100 were achieved with a diverse range of terminal alkynes, excluding sterically unencumbered propargyl-heteroatom derivatives. Our 2013 report was soon followed by the work of Tsuchimoto et al. on the catalysis of DHBTA by zinc triflate with pyridine, which matched the alkyne scope of the (SiNN)Ir catalyst, but required the use of a

diaminoborane HBdan, was not effective with HBpin.[36] Subsequently, our group disclosed[37] that Pd complexes supported by the POCOP pincer ligands were modest DHBTA catalysts while Bertrand et al. showed[38] that copper carbene complexes can catalyze DHBTA with turnover numbers approaching those of the (SiNN)Ir system. Our group's exploration of alternative pincer ligands for the iridium DHBTA system resulted in the finding that Ir complexes of the diarylamido/bis(phosphine) PNP ligands[39,40] act as long-lived and active catalysts, capable of turnover numbers in the thousands.[41]

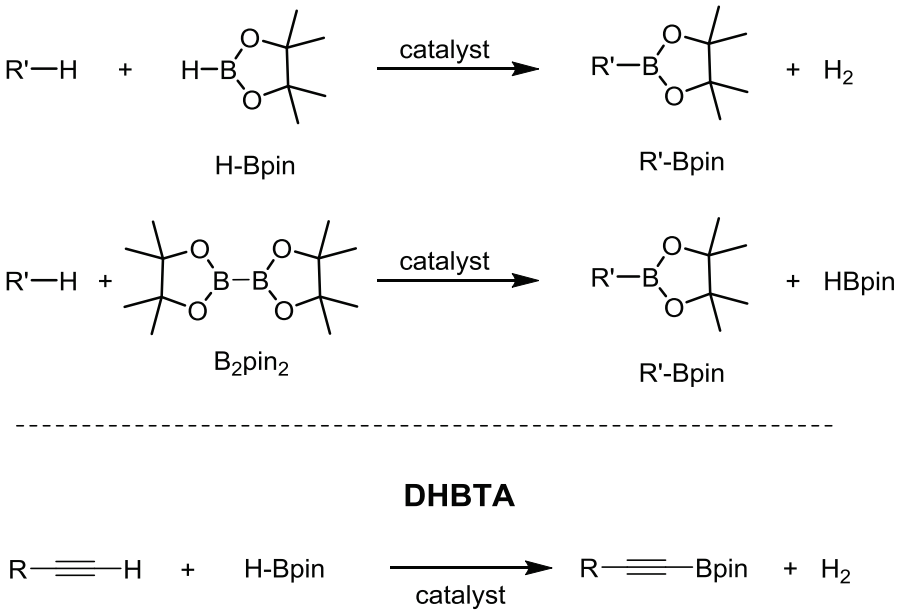

Scheme 1. Top: generic C-H borylation using HBpin or B_2pin_2 reagents; bottom: dehydrogenative borylation of terminal alkynes (DHBTA).

Scheme 2. DHBTA mechanism proposed in reference 35.

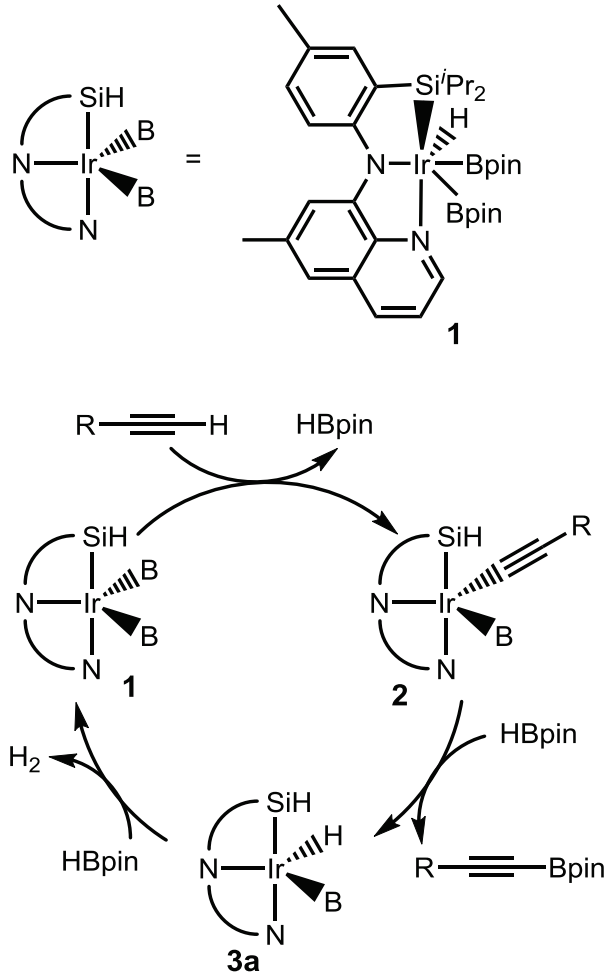

In the 2013 report,[35] a tentative mechanism was conjectured (Scheme 2), largely by analogy with the mechanisms implicated in C-H borylation of arenes catalyzed by Ir complexes supported by bidentate neutral ligands.[3] However, the mere fact that the bipyridine-based catalysts did not catalyze DHBTA while the SiNN complexes of Ir did not catalyze aromatic C-H borylation led us to suspect that the mechanism for DHBTA with the SiNN-based catalyst might not parallel the mechanism accepted for the Ir aromatic C-H borylation catalysts. We also reported on the analogous SiNN complexes of Rh.[42] While the Rh complexes did not catalyze DHBTA, they provided examples of reactivity that highlighted the unusual dual non-innocence of the SiNN ligand with respect to the potential migration of boryl groups from the metal to the amido nitrogen and the adaptability of the nature of the Si-H interaction[43]

with the transition metal center. With these notions in mind, we set out to explore the mechanistic picture in the DHBTA catalysis using DFT calculations. The present work describes our findings that showcase the versatility of the SiNN framework and demonstrate multiple competitive low-energy pathways available in this system for DHBTA. The Ir DHBTA catalysts supported by diarylamido/bis(phosphine) PNP ligands demonstrated[41] much higher turnover numbers than the original SiNN system. However, the limitation of the SiNN system is largely in the catalyst decomposition, but the SiNN system is comparable to the best PNP catalysts in terms of initial rates and is slightly more chemoselective. Thus we thought the understanding of the function of the SiNN system would bring valuable insight and focused on this system.

Results and Discussion.

Parameters of the study. The SiNN catalyst has shown itself capable of borylation of a variety of terminal alkynes carrying aryl, alkyl, and silyl substituents. For this work, we decided to focus on PhCCH as the prototypical alkyne substrate and its conversion to PhCCBpin and H_2 in a catalyzed reaction with HBpin (i.e., R = Ph for DHBTA shown in Scheme 1). For this reaction, ΔG^0_{rxn} was calculated to be -8.2 kcal/mol. Our experimental work showed that **1** is the dominant compound formed in the SiNN system in the presence of excess HBpin. Therefore, our approach was to examine the reaction profile starting from compound **1**.

The Gaussian suite of programs[44] was used for the ab initio electronic structure calculations. All structures were fully optimized by the M06[45] functional with the SDD/6-311G(d,p) basis set in the gas phase, and harmonic vibrational frequency calculations were performed to ensure that either a minimum (for intermediates) or a first-order saddle point (for transition states) was obtained. The solvation energies in benzene at room temperature were calculated on the M06-optimized geometries via the PCM model[46] with the double hybrid dispersion-corrected functional, B2PLYP-D3.[47] The free energies in the following discussion are given relative to the initial reactants (**1** + PhCCH + HBpin), unless otherwise specified.

Note on the depictions of calculated (SiNN)Ir structures. The geometries obtained in this study are quite diverse and do not easily fall along the lines of classical coordination geometries (e.g., octahedral or square pyramidal). Full ball-and-stick representations of each structure, along with the coordinate files can be found in the Supporting Information. Within this text's graphics, we abbreviated the SiNN ligand with simple lines connecting Si-N-N. These abbreviated depictions should not be taken to represent the true stereochemistry about the Ir center. For example, the Si atom is typically not in the same plane as the two nitrogens and the iridium center. To simplify the drawings, we did not separately show bonding between Ir and the H derived from the SiH in the SiNN ligand. Instead, we used "SiH" connected to Ir via a single line. The nature of the actual Ir/Si/H interactions differs significantly

among the presented compounds and the details are discussed separately for selected compounds. In our drawings, the star symbol added to SiH (i.e., SiH) is meant to indicate that the closest Si-H contact exceeds 2.00 Å.*

Initial reaction of 1 with PhCCH via direct OA or 1,2-addition. We first endeavored to analyze the possible outcomes of the reaction of **1** with PhCCH that would lead to the cleavage of the alkynyl C-H bond, which we saw as the requisite initial step in the catalytic cycle. We first examined a conventional oxidative addition (OA) of the C-H bond to the Ir center in **1**; two diastereomeric products could be envisaged (Scheme 3). However, optimizations of the ground state geometries of the products of direct C-H OA to Ir in **1** resulted in structures **4a** and **4b** of unreasonably high energy (+24.9 and +26.5 kcal/mol). Since the transition states leading to **4a**/**4b** would have to be of even higher energy, this pathway overall appeared unlikely and further pursuit along this route was abandoned.

We then contemplated the 1,2-addition of a C-H bond across the Ir-N_{amido} bond[48] (Scheme 3). This notion is based on the previously studied 1,2-additions of C-H bonds in alkynes and arenes Pd-N_{amido} or Pt-N_{amido} bonds in the cationic PNP complexes of Pd and Pt.[49,50] The C-H bonds in those reactions were split with addition of H to N and C to the metal, similarly to **5a** in Scheme 3. The product (**5a**) of the 1,2-addition of the C-H bond of PhCCH to **1** was calculated to lie only 8.3 kcal/mol higher in energy than **1**. We also briefly contemplated the inverse case of 2,1-addition with C connecting to N, but were unable to locate a minimum corresponding to the putative product **5b** of such 2,1-addition.

Scheme 3. Conceivable initial reactions of PhCCH with **1** by C-H OA to Ir or 1,2-addition across Ir-N_{amido}.

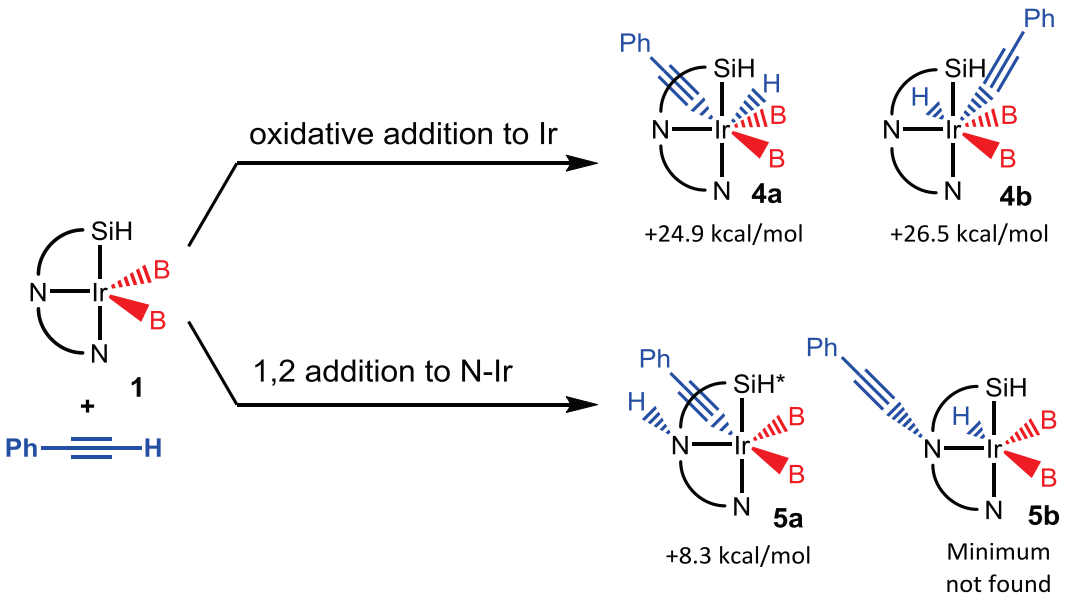

C-B RE from **5a** would result in PhCCBpin and complex **6**, which lies higher in energy, at 15.6 kcal/mol (Chart 1). We have not calculated the TS for this RE process, but assuming it lies yet higher than 15.6 kcal/mol, it may already be non-competitive vs the mechanisms we discuss later. Our calculations, however, indicated that even greater difficulty exists for the subsequent reaction of **6** with HBpin to release H_2 and regenerate **1**; this is needed to complete catalytic turnover. **6** may (Chart 1) be converted to **1** either via addition of HBpin to the Ir center to give **7** followed by loss of H_2, or via isomerization into **3a**, followed by reaction of the latter with HBpin. For the former, addition of HBpin to **6** is exergonic, however **TS7-1** for the 1,2-elimination of H_2 from the resultant compound **7** lies quite high in energy at 26.6 kcal/mol. Ostensibly, part of the reason for the relatively high barrier is that the hydride to be combined with the NH proton in the structure of **7** is not a classical hydride but decidedly a part of a σ-HBpin complex substructure (calculated B-H distance of 1.330 Å).[51-53] On the other hand, the calculated barrier for the migration of H from N to Ir (**TS6-3a**) was also calculated to be surprisingly high at 30.8 kcal/mol. The reaction of **3a** with HBpin is analyzed later in the text, but the 30.8 kcal/mol barrier in Chart 1 to reach **3a** is clearly prohibitive.

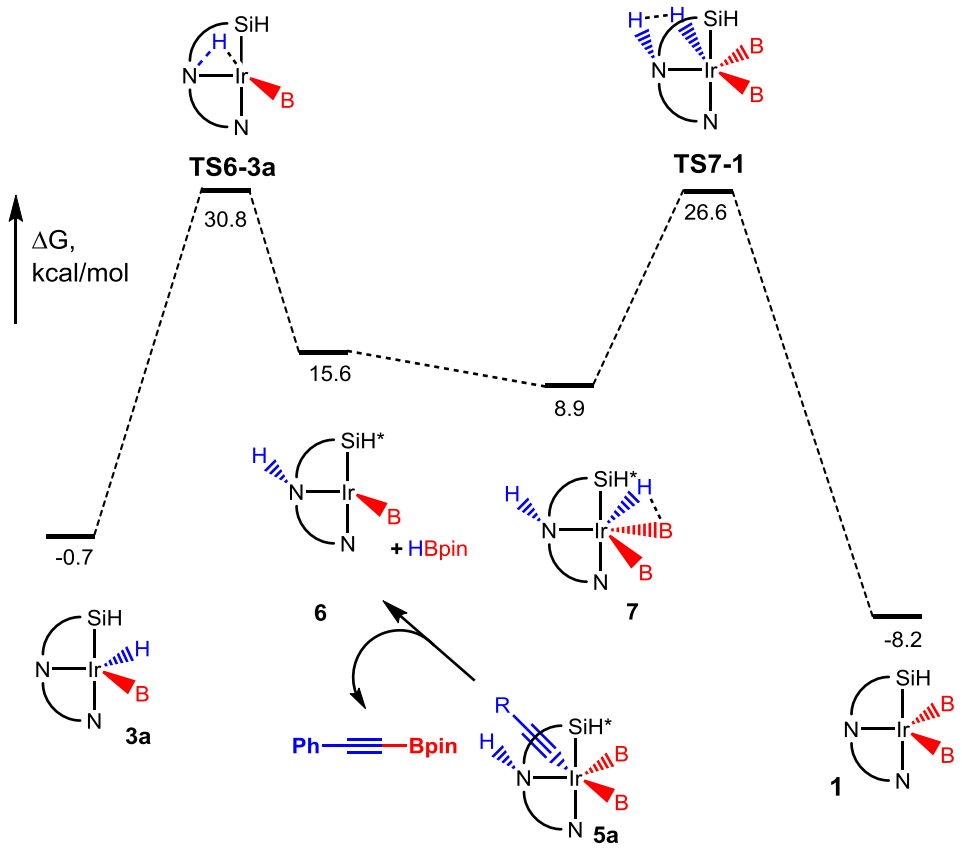

Chart 1. Reaction pathways starting from 1,2-addition of PhCCH across the N-Ir bond in **1**.

It is interesting to point out that direct transfers of a Bpin group between N and Ir appear to proceed with much lower barriers than the analogous migrations of H. It is likely that the presence of an empty π-orbital in N-Bpin or Ir-Bpin and the larger size of B vs H allow for a lower-energy trajectory for the 1,2-migration. However, some caution[54] must be exercised here against the possibility of an alternative mechanism for the net 1,2-migration of H that we have not explicitly analyzed in our calculations. Migration of a proton may be assisted by adventitious bases or perhaps by some of the reactants or products present in solution.

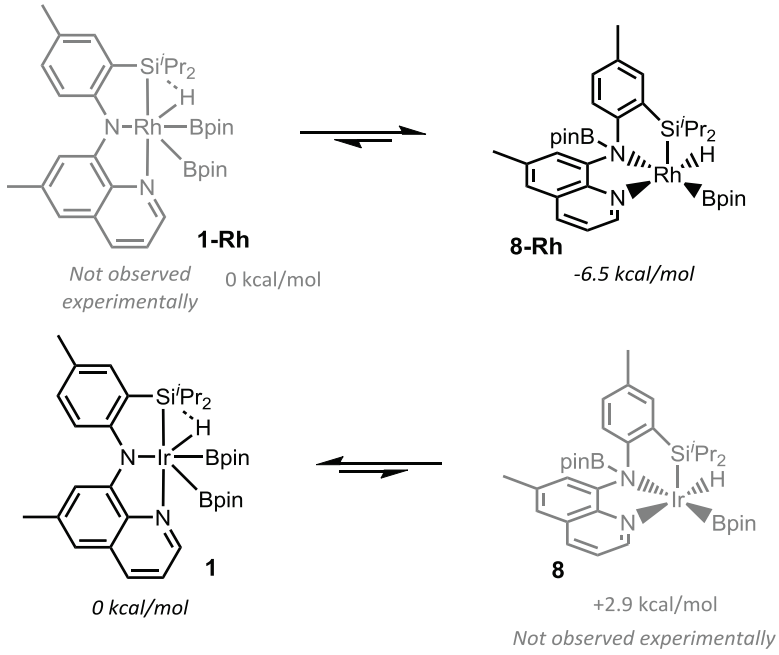

Scheme 4. Isomerization of the diboryl complexes **1** and **1-Rh**.

Mechanisms arising from reactions of 8. Having encountered prohibitively high energy intermediates resulting from direct OA of PhCCH to **1** and prohibitively high energy transition states in pathways derived from 1,2-addition of PhCCH across N-Ir in **1**, we turned our attention to the mechanistic possibilities emanating from the addition of PhCCH that follows isomerization of **1** into complex **8**. The notion of isomerization via boryl migration is based on the experimental observations we made in the SiNN-ligated Rh system (Scheme 4).[42] We recently demonstrated that Rh and Ir have different isomeric preferences for the diboryl complexes – Rh prefers isomer **8-Rh** with one of the boryls on N, whereas Ir prefers a metal/diboryl isomer **1**. However, the other isomer **8** was calculated only slightly higher in energy for Ir and accessible via a modest barrier in the gas phase using the M06 functional. The application of the benzene solvation correction using B2PLYP-D3 (for consistency with the other results in the present work) has resulted in only slight changes in the energies for **TS1-8** (14.1 kcal/mol relative to **1**), the analogous **TS1-8Rh** (11.6 kcal/mol relative to **1-Rh**), compound **8** (2.9 kcal/mol), and compound **8-Rh** (-6.5 kcal/mol relative to **1-Rh**). The investigation of these possibilities has revealed a complex web of interlinked reactions offering multiple mechanistic options with comparably low barriers for achieving catalytic turnover. Scheme 5 presents this web as a composite

graphic of sevral Parts for the discussion that follows. It contains three cycles (**I**, **II**, and **III**) each split into two halves (denoted **-a** and **-b**) and three auxiliary transformations denoted **X**, **Y**, **Z**.

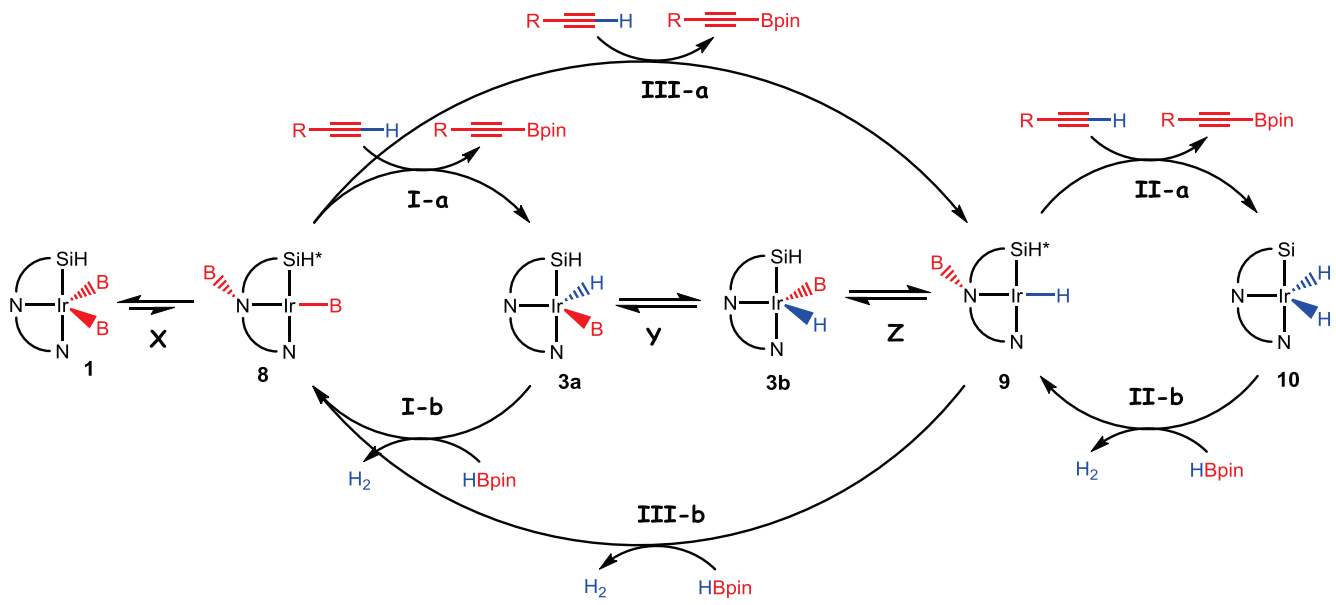

Scheme 5. Summary of reaction pathways derived from compound **8**.

Parts X and I-a. Isomerization of **1** to **8** (Part **X** in Scheme 5) was discussed above (Scheme 4). For Part **I-a** (Chart 2), OA of PhCCH to **8** was found to lead to compound **11a**[55] at +8.9 kcal/mol relative to **1**. The **TS8-11a** energy[56] for this OA is modest at 12.1 kcal/mol vs **1**, i.e., slightly lower than the TS for the isomerization of **1** into **2**. The relative favorability and facility of OA of PhCCH to **8** vs the direct OA of PhCCH to **1** can be rationalized by considering that migration of the boryl ligand from Ir to N (i.e., **1→8**) is effectively B-N reductive elimination (RE). Although differentiation between **1** and **8** in terms of formal oxidation states is obscured by the changes in the bonding within the Ir/Si-H triangle,[42] it is nonetheless clear that boryl migration onto the lone pair at N leaves behind a lone pair at Ir. In addition, boryl migration also decreases the coordination number at Ir. Thus, the Ir center in **8** is better suited for undergoing OA compared to **1**. The barrier to the migration of the boryl ligand from Ir to N is

rather modest, which could be attributed to the orbital correlation between N and boryl ligand, as shown in Chart 2 for the corresponding **TS1-8**. During the migration, N behaves as a Lewis base, with a lone pair of electron in its 2p orbital, while B of the N-Bpin moiety is a typical Lewis acid, having an empty p orbital. The Lewis base and Lewis acid interaction facilitates the formation of the new B-N σ bond and the breaking of the existing B-Ir bond, meanwhile transforming the N_{amido}-Ir bond in **1** into the N_{amine}→Ir dative bond in **8**.

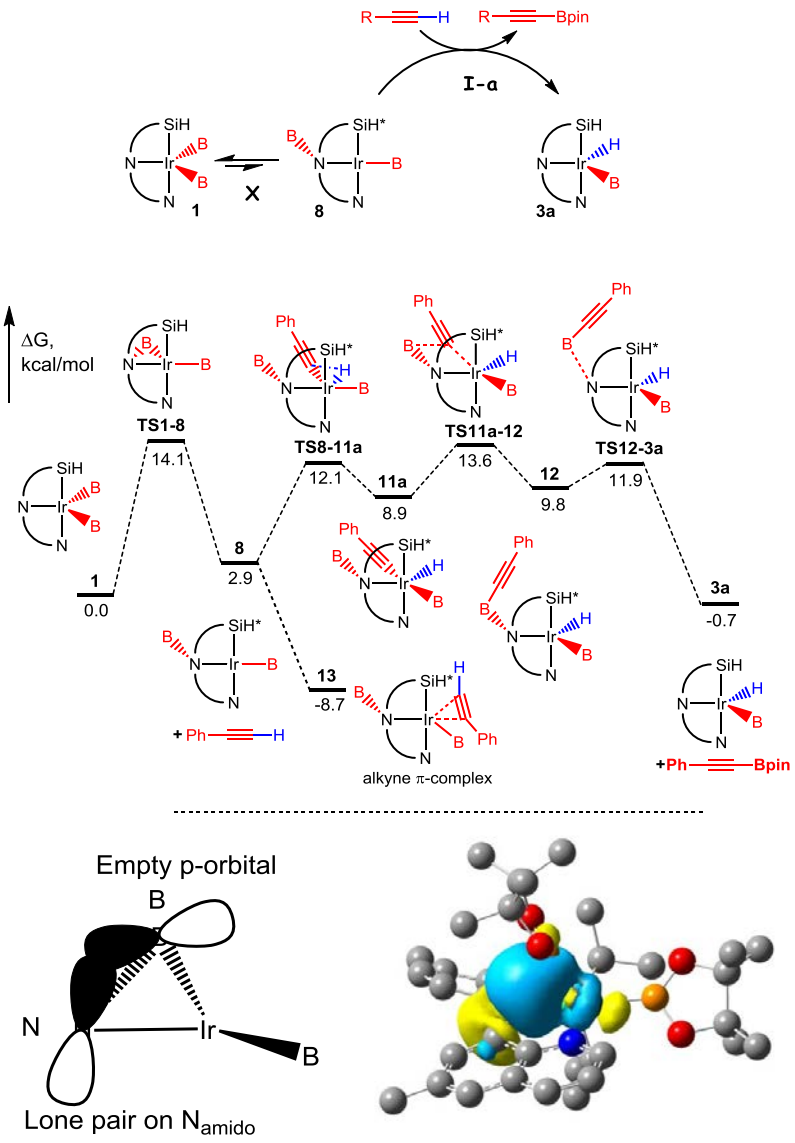

Chart 2. Top: Parts **X** and **I-a**. Bottom: Generic orbital correlation and the calculated orbitals for the Bpin migration (**TS1-8**).

Next, we turned our attention to the formation of the B-C bond of the alkynylboronate product, starting from intermediate **11a** (Chart 2). We found a rather unusual, low-energy pathway for B-C bond formation via **TS11a-12** resulting in intermediate **12**. Intermediate **12** is merely a weak adduct of the alkynylboronate product with the lone pair of the amido ligand and its dissociation is facile (via **TS12-3a**), leading to the free alkynylboronate and complex **3a**. **TS11a-12** represents the carbon-boron bond-forming step. This process is not at all an RE from the metal; it rather has to be viewed as a 1,2-migration of the alkynyl anion (Lewis base) to the empty orbital of the nitrogen-bound Bpin group (Lewis acid).

The structure of the product of addition of PhCCH to the Ir center in **8** with the formation of a η^2-PhCCH π-complex was also calculated (compound **13**; it lies -8.7 kcal/mol below the reactants. This suggests that **13** might be the resting state of the catalyst. Furthermore, the existence of **13** adds a significant 8.7 kcal/mol to the effective overall barrier for the transformation. Thus, a barrier of merely 10.7 kcal/mol (**TS11a-12** vs **8**)[57] becomes a barrier of 22.3 kcal/mol relative to **13**. Experimental studies to rigorously determine the experimental energy of activation have not been carried out, but considering that 100 turnovers were observed to be completed in 10 min or less,[35] an apparent activation energy of 17-19 kcal/mol can be estimated. However, it should be noted that the formation of π-adduct analogs of **13** with ^{n}BuCCH and Me_3SiCCH was calculated to be less favorable (-4.7 and -5.4 kcal/mol, respectively)[58] and it is possible that the calculations overestimate the stability of **13** due to the competition of various π-π stacking interactions between SiNN, PhCCH, and benzene solvent.

Part I-b. Part **I-a** described the conversion of compound **8** and PhCCH into the PhCCBpin product and compound **3a**. To complete the catalytic cycle, compound **3a** must then react with free HBpin to regenerate complex **8** and produce free H_2. The calculated pathway for this transformation is depicted in Chart 3 and proceeds with a modest barrier corresponding to the **TS3a-14** of the initial addition of HBpin to the N lone pair in **3a**. The transfer of hydride from the B-H moiety in **14** to the Ir center results in the formation of **15**. Subsequent loss of H_2 from **15** via a dihydrogen complex **16** also appears

to be very facile. The energy of **TS3a-14** is 9.5 kcal/mol relative to **1**+PhCCH+HBpin (or 10.2 kcal/mol relative to **3a** + HBpin or 18.2 kcal/mol relative to **13**), and thus below the highest TS in Part **I-a** and the overall barrier for Cycle **I** thus remains 22.3 kcal/mol.

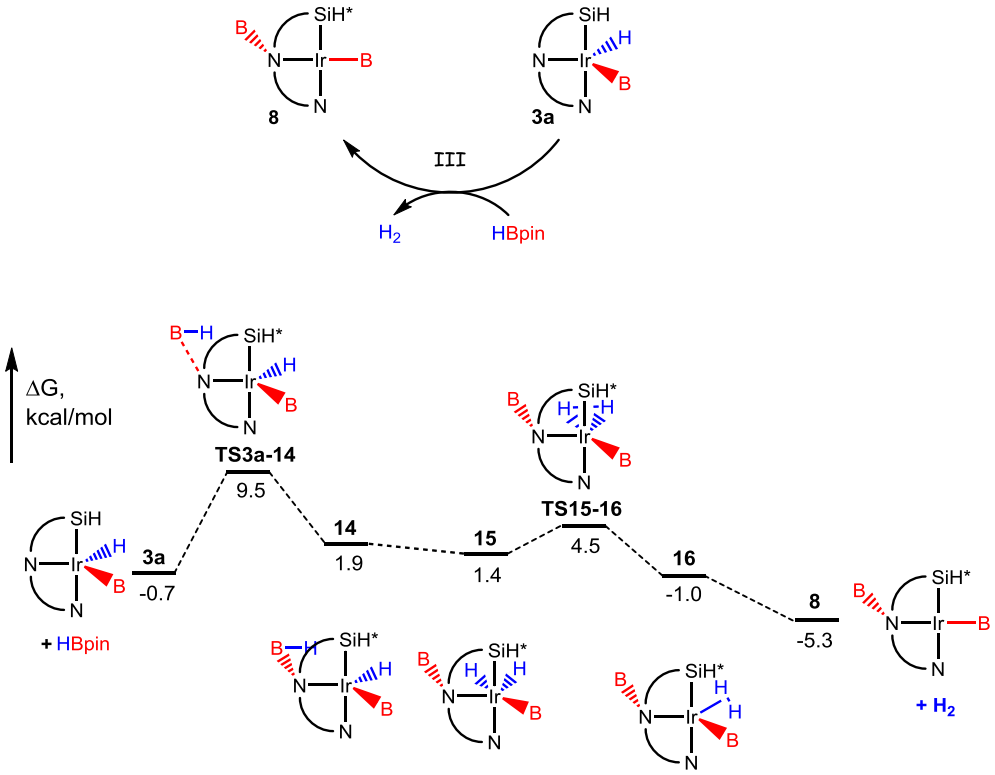

Chart 3. Part **I-b**: reaction of **3a** with HBpin to produce free H_2 and **8**.

Parts Y, Z, and II-a. If Part **I-a** represents a viable pathway, then compound **3a** is available in the reaction mixture as an intermediate in the catalytic cycle. As such an intermediate, **3a** is produced as a result of a favorable reaction. In addition, Part **I-b** in reverse (i.e., **8** + **H_2** → **3a**) provides an alternative reaction, albeit unfavorable, to access compound **3a** in the reaction mixture once some H_2 is generated as a result of the DHBTA catalysis via Cycle **I**. By this route, **3a** would lie 4.6 kcal/mol above **8** + H_2, and thus 7.5 kcal/mol above **1** + H_2 with the barrier of 14.8 kcal/mol (**TS3a-14**) relative to **8** + H_2, which is higher than the barrier for compound **8** to proceed in the forward direction of Cycle I.

The realization of the inevitable presence or accesibility of **3a** in the reaction mixture led us to consider whether a "monoboryl" pathway may also be viable analogously to the "diboryl" Cycle **I**. In the formation of PhCCBpin in Part **I-a**, the Bpin ligand attached to Ir is not engaged in the product bond formation. Thus it was envisaged that an Ir-bound hydride in **3a** may support similar transformations via Cycle **II**.

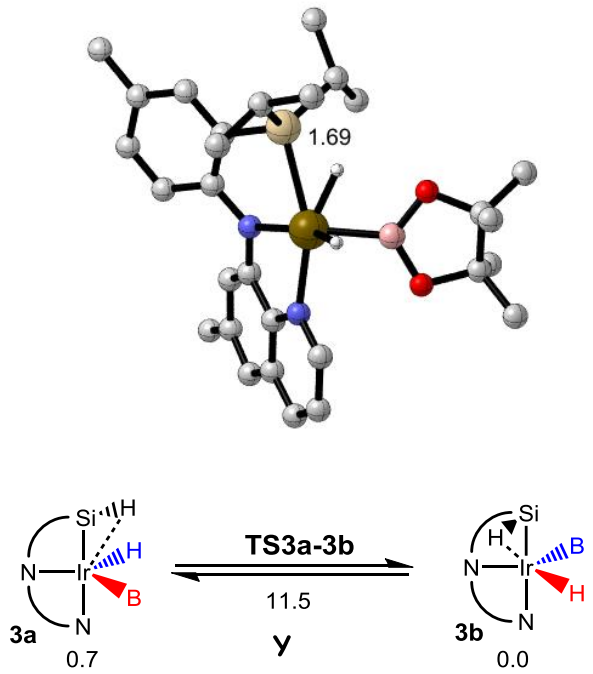

Chart 4. Part **Y**: the **3a/3b** isomerization and the geometry of the **TS3a-3b**. ΔG values are given relative to compound **3b** at 0 kcal/mol.

At first, we analyzed the isomerization of **3a** into **3b**, which would be the necessary diastereromer for facile Bpin migration from Ir to N. The isomerization (Part **Y**, Chart 4) is nearly isoergic, favoring **3b** by merely 0.7 kcal/mol, and proceeds with a low barrier of 10.8 kcal/mol relative to **3a**. Thus, if **3a** is kinetically accessible in this system, **3b** should be accessible, as well. In **3a** and **3b**, the IrNN plane bisects the Si-H vector, as well as the B-H vector. The difference between these two isomers is in that in **3a** the two H's lie to the same side of the IrNN plane, while they are on the opposite sides in **3b**. The isomerization proceeds via movement of the SiH hydrogen across the IrNN plane with the **TS3a-3b**

possessing the metrics of an Si-H σ-complex with a shorter Si-H distance (1.69 Å) than in **3a** or **3b** (Figure 2).

The examination of the Bpin migration from Ir in **3b** to N (Part **Z**, Chart 5), to give a new complex **9**, revealed that it is slightly less endergonic (1.1 kcal/mol for **9** vs **3b**) and more facile (10.6 kcal/mol barrier, **TS3b-9**) than the analogous Bpin migration in the conversion of **1** to **8**. The subsequent steps (Part **II-a**) of OA of PhCCH to the Ir center to give **17** and the migration of the alkynyl onto the N-bound boron to give **18** with subsequent release of free PhCCBpin and generation of intermediate **10** were also found to proceed similarly to the "diboryl" pathway in Part **I-a**, but with slightly lower barriers. The π-complex **19** here was calculated to be less favorable of an adduct than in the case of **13**.

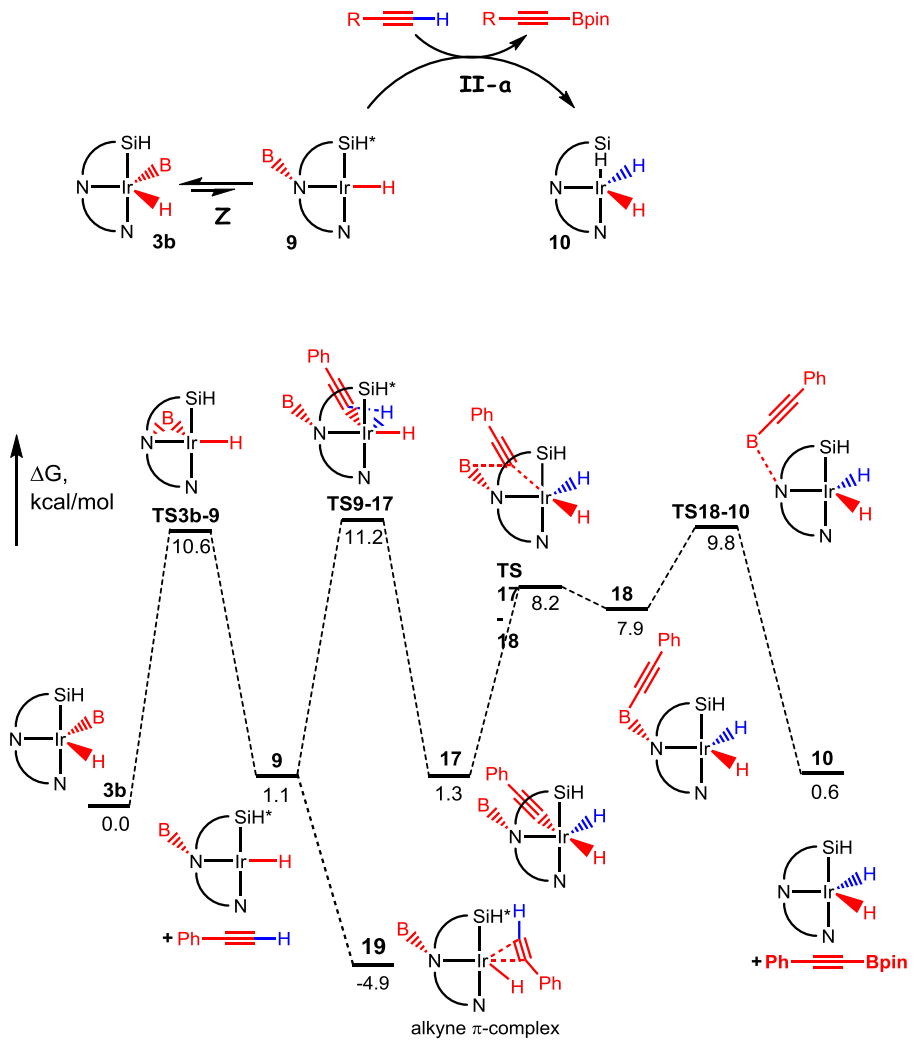

Chart 5. Parts **Z** and **II-a**: the "monoboryl" pathway for PhCCBpin formation.

Table 1. Selected distances (in Å) in the calculated structures of **1**, **3a, 3b**, and **10**.

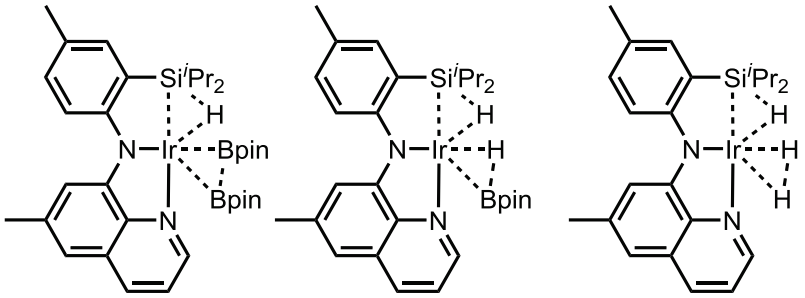

Bond/Compound	1	3a	3b	10
Si-H	1.889	1.956	1.966	1.999
Ir-Si	2.452	2.423	2.383	2.381
Ir-H$_{Si}$	1.609	1.606	1.599	1.601
B-B	2.196	–	–	–
B-H	–	1.551	1.538	–
H-H	–	–	–	1.503
Ir-B	2.064 2.055	2.058	2.072	–
Ir-H$_{B/H}$	–	1.645	1.644	1.599 1.582

It is interesting to contemplate the similarity among the structures of **1, 3a, 3b, and 10**. All four of them possess the SiNN ligand in addition to a pair of X/Y donors where X and Y are H or Bpin, with a very similar disposition of these ligands relative to each other about Ir. The binding of the Si-H from the SiNN ligand on one hand, and of the H-H/H-B/B-B on the other can in principle be analyzed either as a σ-complex or as product of OA, with two classical X-type ligands. Inspection of the calculated interatomic distances (Table 1) in the two corresponding triangles (Ir/Si/H and Ir/X/Y were X, Y = B or H) in these four molecules reveals that, broadly speaking, both triangles are close to the divide between a σ-complex and an OA structure. The Si-H distances are in the 1.9-2.0 Å range, which is essentially where the divide is often postulated, perhaps slightly inside the σ-complex range.[43] The H-H distance of 1.503 Å in **10** is at the edge of range of distances that has been posited the so-called compressed

dihydrides.[59,60] The B-H distances in **3a** and **3b** and the especially the B-B distance in **1** are more firmly in the range expected for neighboring classical boryls and hydrides.[51-53] The Si-H distance decreases upon successively replacing the H-H partner with B-H and then with B-B. This can be interpreted as OA of B-B being "more complete" than that of H-H, resulting in less back-donation into the Si-H bond in **1** vs **10**, with **3a**/**3b** presenting an intermediate situation. Dovetailing a previously published discussion,[42] this illustrates the subtle adaptability of the SiNN ligand in response to various changes at the metal center.

Part II-b. To complete the "monoboryl" catalytic Cycle **II**, the generation of H_2 from the reaction of **10** with HBpin was approached next (Part **II-b**, Chart 6). The energies along the pathway of Part **II-b** were found to be lower relative to **10** than were the analogous energies in Pathway **I-b** relative to compound **3a**. On the other hand, compound **20** turned out to be lower in energy than **10** (+ HBpin), whereas the analogous compound **15** in Part **I-b** is higher in energy than **3a** + HBpin. Therefore, **20** is the lowest energy compound in the "monoboryl" Cycle **II** relative to [**3a** + HCCPh + HBpin]. However, the barrier to go from **20** over **TS9-17** in the forward direction of Cycle **II** is 11.2 – (-6.1) – 8.2 = 9.1 kcal/mol because of the intervening favorable product formation. Thus the effective barrier for Cycle **II** is determined by the difference in energy between **TS9-17** and **19**, resulting in 16.1 kcal/mol. This is markedly smaller than the difference between **TS11a-12** and **13** of 22.3 kcal/mol and more in line with the observed experimental rates.

The whole situation is rather complex. As mentioned previously, **3a** can be favorably produced in the natural course of Part **I-a** or unfavorably and with a relatively high barrier from **8** + H_2. The barrier for **3a** to proceed along Part **II-b** (Chart 3) to react with HBpin and produce **8** is 10.2 kcal/mol. On the other hand, the barrier for **3a** to isomerize into **3b** is 10.8 kcal/mol and the subsequent TS energies along Parts **Z**, and then **II-a** and **II-b** are lower. If these small differences in numbers are taken at face value, Cycle **II** does possess a lower barrier for catalytic turnover, but **3a** needs Cycle **I** to be favorably generated and is more likely to complete Cycle **I** than to "switch" to Cycle **II**.

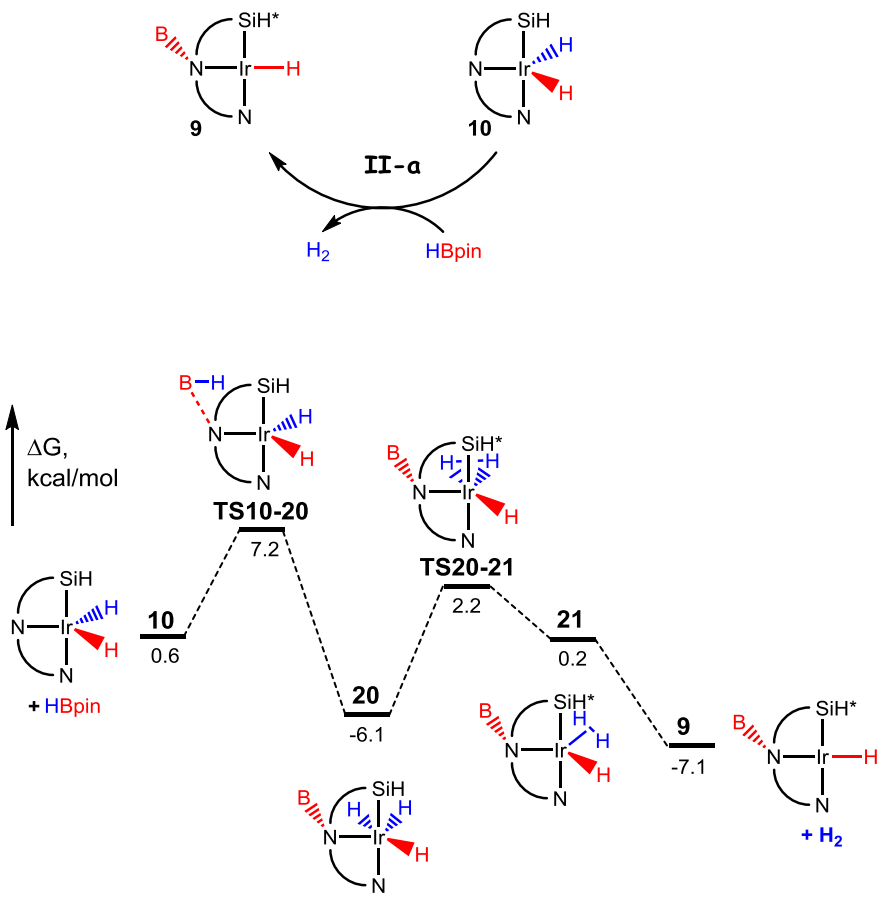

Chart 6. Part **II-b**: the "monoboryl" pathway for H_2 generation.

Parts III-a and III-b. Having examined the pathways (Parts **I-a** and **II-a**) in which the C-B bond formation proceeded via migration of alkynyl from Ir onto an N-bound boron, we decided to delve more closely into the possibility of a more conventional C-B RE from Ir following OA of the C-H bond of PhCCH to **8** (Chart 7). In Part **I-a**, we considered complex **11a** as the product of that OA. However, there are at least a few distinct diastereomers of **11a**. Some of these may be formed as immediate products of PhCCH OA, while others may be accessible by subsequent isomerization. The isomeric structures **11a-d** can be viewed as possessing very similar mutual dispositions of the alkynyl and the two nitrogenous donors (C, N, N' in Figure 1) and differing in the arrangement of the Si, B, and the two H atoms about Ir. Based on the corresponding interatomic distances (Table 2), the structures of **11b-d** are best analyzed as approximately octahedral, with one site being occupied by an H-H (**11b**) or Si-H (**11c** and **11d**) σ-complex. The H-H distance in **11b** positions it among the "normal", not "stretched"

dihydrogen complexes.[59,60] The Si-H distances of slightly over 1.8 Å in **11c** and **11d** fall within the range of silane σ-complexes.[43] Structure **11a** is best viewed as a pentagonal bipyramid with an Ir(V) formulation. The closest candidate for a σ-complex assignment is the B-H contact, but at 1.603 Å this is generally longer than is typically treated within the σ-complex formalism.[51-53] It is possible that there are other isomeric minima in this system that we have not considered. However, given that the barriers that we have calculated among **11a-d** are all very small (and **11b→11c** is barrierless), any other isomer is likely to also be accessible via an insignificant barrier.

With respect to the catalytic process at hand (Chart 7), the key finding is that isomer **11d** is readily available via low-barrier transformations following OA of PhCCH to **8**. Compared to **11a**, isomer **11d** positions the alkynyl PhCC ligand next to the Ir-bound BPin ligand and RE of PhCCBpin from **11d** is very facile with the **TS11d-9** lying only 3.6 kcal/mol above **11d**.

Table 2. Selected interatomic distances (in Å) in the calculated structures of **11a-d**.

Bond/Compound	11a	11b	11c	11d
Si···H[a]	2.837	2.459	1.823	1.817
B···H[b]	1.603	2.445	2.326	2.100
H···H	2.058	0.914	1.696	2.306

[a] The distance for the closest Si···H contact given. [b] The distance for the closest B···H contact given.

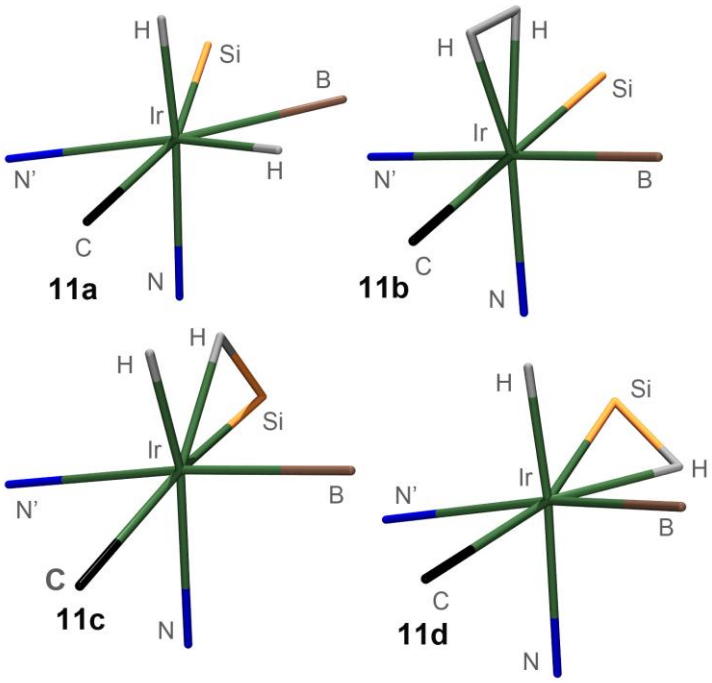

Figure 1. Structures showing the immediate coordination environment about Ir in compounds **11a-d**. N' indicates the nitrogen attached to one of the Bpin groups.

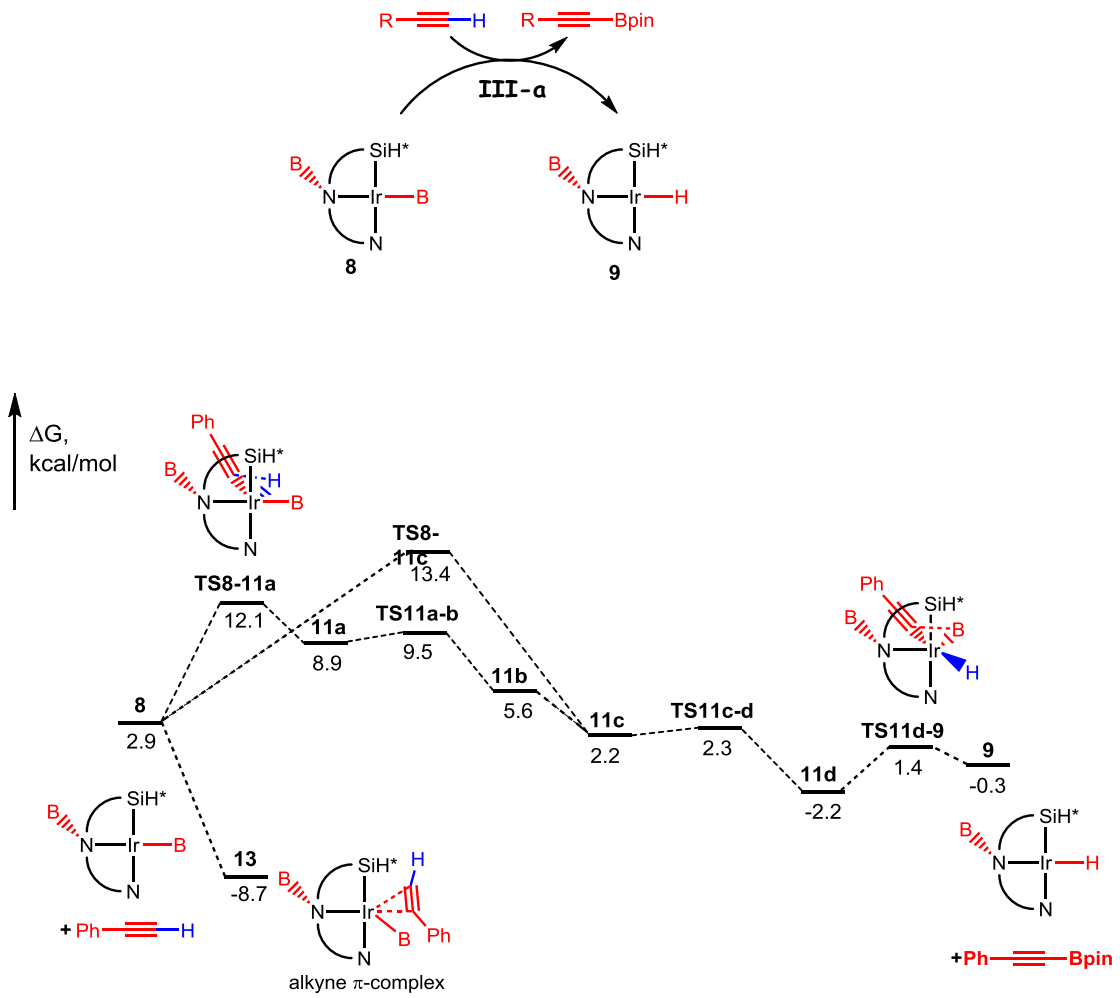

Chart 7. Part **III-a**: the "diboryl" pathway with C-B RE from Ir.

To close Cycle **III**, compound **9** has to be converted to **8** and H_2 in a reaction with HBpin. Chart 8 details this pathway (Part **III-b**), which possesses a very smooth reaction coordinate. Overall, Cycle **III** possesses a barrier of 20.8 kcal/mol (the difference between **TS8-11a** and compound **13**). This is 1.5 kcal/mol lower than for Cycle **I** because Cycle **III** avoids having to go via **TS11a-12**, which lies 1.5 kcal/mol higher than the highest point of Cycle **III** (**TS8-11a**). And although the 20.8 kcal barrier for Cycle **III** is higher than the barrier in the "monoboryl" Cycle **II**, it does not rely on **3a** "avoiding" the slightly more facile Part **I-b** in order to engage in Cycle **II**.

Although Part **III-b** can be viewed as isomeric to Part **I-b**, it is not the same process since Part **I-b** starts with complex **3a** (boron on Ir), whereas Part **III-b** starts with its isomer **9** (boron on N). Compounds **3a** and **9** can of course interconvert via **3b** (Parts **Y** and **Z**). In addition, since **8** is an intermediate in Part **I-a** and **9** is an intermediate in Part **II-a**, this illustrates that all three catalytic cycles we have examined have points of intersection.

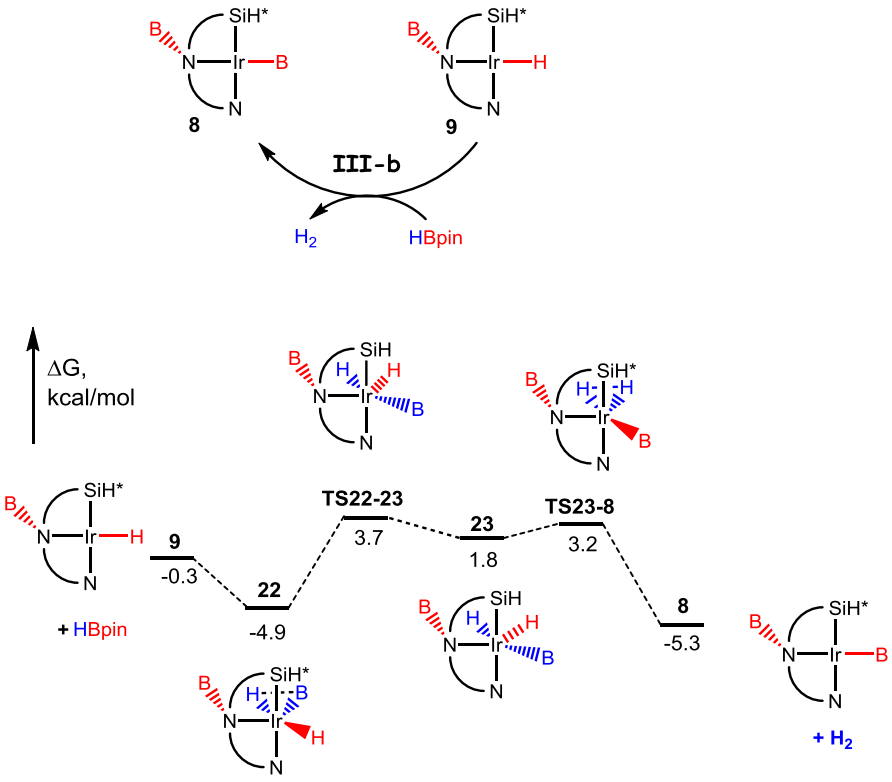

Chart 8. Part **III-b**: Reaction of **9** with HBpin to release H_2.

Conclusion

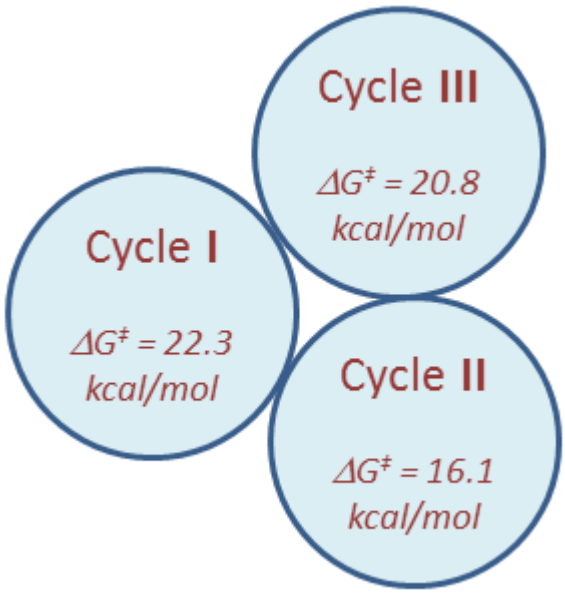

Figure 2. Simplified representation of the three intersecting catalytic cycles with the intra-cycle free energy barriers shown.

Judging each of the three catalytic cycles individually (Figure 2), Cycle **II** appears to have the lowest barrier as judged by the smallest difference between the lowest energy participating compound and the highest energy TS. However, this cycle can only be accessed starting with compounds **3a**/**3b**/**9**, which require either endoergic formation from **1** or **8** and H_2 (thus rendering Cycle **II** higher in energy) or formation via execution of Part **I-a** or Part **III-a**, which are exoergic processes. Both Part **I-a** and Part **III-a** rely on the same C-H OA step (**TS8-11a**) but Part **III-a** provides a lower-barrier route for C-B bond formation via RE from Ir as opposed to the unusual alkynyl migration from Ir to B in Part **I-a** (and in Part **II-a**). However, the differences among the barriers in different cycles do not amount to more than a few kcal/mol and the differences among multiple TS within each cycle are similarly small. The fact that the various cycles have common intermediates and the system can thus "jump" from one cycle to another further complicates the picture. It would be naïve to think that DFT calculations can resolve and provide confident relative ranking of so many possibilities with such a narrow range of energies.

Furthermore, the experimental system would be complicated by the evolving concentrations of the reagents (HBpin and PhCCH) and products (PhCCBpin and H_2) in the course of the reaction, since these may influence the relative concentrations of the various intermediates. Lastly, given the small calculated differences here with PhCCH as the model substrate, it is certainly possible that different cycles prevail for different alkynes.

Nonetheless, it is clear that the uncertainty in this system stems precisely from the fact that multiple pathways are available at similarly low energies. Providing low-energy pathways is precisely the intent of catalyst design and the process may only benefit from the availability of multiple pathways that can plausibly accomplish the same net reaction goal. In the case under study here, it is the two "non-innocent" features of the SiNN supporting ligand that are responsible for the great variety of options. Firstly, the availability of the amido ligand and its lone pair provides for facile migration of the boryl ligand between Ir and N. Secondly, the adaptability of the mode of interaction of the Si-H unit with Ir, varying from a moderately perturbed Si-H σ-complex to full Si-H oxidative addition to Ir provides significant flexibility in accommodating changes at the Ir center in the progression of the various cycles.

The more recently reported PNP-based Ir catalysts for DHBTA do not possess an adaptable Si-H moiety, so clearly the presence of Si-H is not a necessary feature of DHBTA catalyst design with Ir. Although the present work has identified several plausibly competitive mechanisms, they all utilize the amido nitrogen in the SiNN ligand for boryl group migration, whereas the changes in the Si-H/Ir bonding are not pronounced in each mechanistic option. This may support the notion that the presence of an amido ligand is a more important design element and that the SiH moiety may be adequately replaced by other ligand functionalities.

Acknowledgment. We are grateful for the support of this work by the US National Science Foundation (grants CHE-1300299 and CHE-1565923) and the National Natural Science Foundation of China (No. 51602079 to J. Z.).

Supporting Information Available. Coordinate files, listings of energy values, and pictorial depictions of the calculated structures. This material is available via the Internet free of charge at http://pubs.acs.org.

References

[1] Cho, J.-Y.; Tse, M. K.; Holmes, D.; Maleczka, R. E., Jr.; Smith, M. R., III. *Science* **2002**, *295*, 305.

[2] Ishiyama, T.; Takagi, J.; Ishida, K.; Miyaura, N.; Anastasi, N. R.; Hartwig, J. F. *J. Am. Chem. Soc.* **2002**, *124*, 390-391.

[3] Mkhalid, I. A. I.; Barnard, J. H.; Marder, T. B.; Murphy, J. M.; Hartwig, J. F. *Chem. Rev.* **2010**, *110*, 890-931.

[4] Hartwig, J. F. *Acc. Chem. Res.* **2012**, *45*, 864-873.

[5] Hartwig, J. F. *Chem. Soc. Rev.* **2011**, *40*, 1992-2002.

[6] Hartwig, J. F. *J. Am. Chem. Soc.* **2016**, *138*, 2-24.

[7] Hall, D. G. *Boronic Acids: Preparation and Applications in Organic Synthesis, Medicine and Materials*, 2nd ed.; Wiley-VCH: Weinheim, 2012.

[8] Preshlock, S. M.; Ghaffari, B.; Maligres, P. E.; Krska, S. W.; Maleczka, R. E.; Smith, M. R. *J. Am. Chem. Soc.* **2013**, *135*, 7572-7582

[9] Boebel, T. A.; Hartwig, J. F. *J. Am. Chem. Soc.* **2008**, *130*, 7534−7535.

[10] Ghaffari, B.; Preshlock, S. M.; Plattner, D. L.; Staples, R. J.; Maligres, P. E.; Krska, S. W.; Maleczka, R. E.; Smith, M. R. *J. Am. Chem. Soc.* **2014**, 136, 14345-14348.

[11] Wang, G.; Xu, L.; Li, P. *J. Am. Chem. Soc.* **2015**, 137, 8058-8061.

[12] Press, L. P.; Kosanovich, A. J.; McCulloch, B. J.; Ozerov, O. V. *J. Am. Chem. Soc.* **2016**, *138*, 9487-9497.

[13] Obligacion, J. V.; Semproni, S. P.; Chirik, P. J. *J. Am. Chem. Soc.* **2014**, *136*, 4133-4136.

[14] Schaefer, B. A.; Margulieux, G. W.; Small, B. L.; Chirik, P. J. *Organometallics* **2015**, *34*, 1307-1320.

[15] Obligacion, J. V.; Bezdek, M. J.; Chirik, P. J. *J. Am. Chem. Soc*. **2017**, *139*, 2825-2832.

[16] Obligacion, J. V.; Chirik, P. J. *ACS Catal*. **2017**, *7*, 4366-4371.

[17] Furukawa, T.; Tobisu, M.; Chatani, N. *J. Am. Chem. Soc*. **2015**, 137, 12211-12214.

[18] Dombray, T.; Werncke, C. G.; Jiang, S.; Grellier, M.; Vendier, M.; Bontemps, S.; Sortais, J.-B.; Sabo-Etienne, S.; Darcel, C. *J. Am. Chem. Soc*. **2015**, *137*, 4062-4065.

[19] Mazzacano, T. J.; Mankad, N. P. *J. Am. Chem. Soc*. **2013**, *135*, 17258-17261.

[20] Legere, M.-A.; Courtemanche, M.-A.; Rochette, E.; Fontaine, F.-G. *Science* **2015**, *349*, 513-516.

[21] Chen, H.; Schlecht, S.; Semple, T. C.; Hartwig, J. F. *Science*, **2000**, *287*, 1995.

[22] Murphy, J. M.; Lawrence, J. D.; Kawamura, K.; C. Incarvito, and J. F. Hartwig, *J. Am. Chem. Soc*. **2006**, *128*, 13684.

[23] Chen H.; Hartwig, J. F. *Angew. Chem. Int. Ed*., **1999**, *38*, 3391.

[24] Brown J. M.; Lloyd-Jones, G. C. *J. Am. Chem. Soc*. **1994**, *116*, 866.

[25] Coapes, R. B.; Souza, F. E. S.; Thomas, R. L.; Hall, J. J.; Marder, T. B. *Chem. Commun*. **2003**, 614.

[26] Ishiyama, T.; Ishida, K.; Takagi, J.; Miyaura, N. *Chem. Lett*. **2001**, *30*, 1082.

[27] Olsson V. J.; Szabó, K. J. *Angew. Chem. Int. Ed*. **2007**, *46*, 6891.

[28] Larsen, M. A.; Cho, S. H.; Hartwig, J. F. *J. Am. Chem. Soc*. **2016**, *138*, 762-765.

[29] Larsen, M. A.; Wilson, C. V.; Hartwig, J. F. *J. Am. Chem. Soc*. **2015**, *137*, 8633-8643.

[30] Ogawa, D.; Li, J.; Suetsugu, M.; Jiao, J.; Iwasaki M.; Nishihara, Y. *Tetrahedron Lett*. **2013**, *54*, 518.

[31] Ishida, N.; Murakami, M. *Top. Organomet. Chem.* **2015**, *49*, 93-116.

[32] León, T.; Fernández, E. *Chem. Commun*. **2016**, *52*, 9363-9366.

[33] Jiao, J.; Nishihara, Y. *J. Organomet. Chem*. **2012**, *721-722*, 3-16.

[34] Lee, C.-I; Shih, W.-C.; Zhou, J.; Reibenspies, J. H.; Ozerov, O. V. *Angew. Chem., Int. Ed*. **2015**, *54*, 14003-14007.

[35] Lee, C.-I; Zhou, J.; Ozerov, O. V. *J. Am. Chem. Soc.* **2013**, *135*, 3560-3566.

[36] Tsuchimoto, T.; Utsugi, H.; Sugiura, T.; Horio, S. *Adv. Synth. Catal.* **2015**, *357*, 77–82.

[37] Pell, C. J.; Ozerov, O. V. *Inorg. Chem. Front.* **2015**, *2*, 720-724.

[38] Romero, E. A.; Jazzar, R.; Bertrand, G. *Chem. Sci*. **2017**, *8*, 165-168.

[39] Ozerov, O. V. "Rigid PNP pincer ligands and their transition metal complexes". In *The Chemistry of Pincer Compounds*; Morales-Morales, D., Jensen, C., Eds.; Elsevier: Amsterdam, 2007; pp 287-309

[40] Davidson, J. J.; DeMott, J. C.; Douvris, C.; Fafard, C. M.; Bhuvanesh, N.; Chen, C.-H.; Herbert, D. E.; Lee, C.-I; McCulloch, B. J.; Foxman, B. M.; Ozerov, O. V. *Inorg. Chem*. **2015**, *54*, 2916-2935.

[41] Lee, C.-I; DeMott, J. C.; Pell, C. J.; Christopher, A.; Zhou, J.; Bhuvanesh, N.; Ozerov, O. V. *Chem. Sci.* **2015**, *6*, 6572-6582.

[42] Lee, C.-I; Hirscher, N. A.; Zhou, J.; Bhuvanesh, N.; Ozerov, O. V. *Organometallics* **2015**, *34*, 3099-3102.

[43] For reviews on the general aspects of bonding between Si-H bonds and transition metals, see: (a) Corey, J. Y. *Chem. Rev.* **2011**, 111, 863– 1071. (b) Nikonov, G. I.*Adv. Organomet. Chem.* **2005**, 53, 217– 309. (c) Alcaraz, G.; Sabo-Etienne, S.*Coord. Chem. Rev.* **2008**, 252, 2395–2409.

[44] Frisch, M. J.; Trucks, G. W.; Schlegel, H. B.; Scuseria, G. E.; Robb, M. A.; Cheeseman, J. R.; Scalmani, G.; Barone, V.; Mennucci, B.; Petersson, G. A.; Nakatsuji, H.; Caricato, M.; Li, X.; Hratchian, H. P.; Izmaylov, A. F.; Bloino, J.; Zheng, G.; Sonnenberg, J. L.; Hada, M.; Ehara, M.;

Toyota, K.; Fukuda, R.; Hasegawa, J.; Ishida, M.; Nakajima, T.; Honda, Y.; Kitao, O.; Nakai, H.; Vreven, T.; Montgomery. Jr., J. A.; Peralta, J. E.; Ogliaro, F.; Bearpark, M.; Heyd, J. J.; Brothers, E.; Kudin, K. N.; Staroverov, V. N.; Kobayashi, R.; Normand, J.; Raghavachari, K.; Rendell, A.; Burant, J. C.; Iyengar, S. S.; Tomasi, J.; Cossi, M.; Rega, N.; Millam, N. J.; Klene, M.; Knox, J. E.; Cross, J. B.; Bakken, V.; Adamo, C.; Jaramillo, J.; Gomperts, R.; Stratmann, R. E.; Yazyev, O.; Austin, A. J.; Cammi, R.; Pomelli, C.; Ochterski, J. W.; Martin, R. L.; Morokuma, K.; Zakrzewski, V. G.; Voth, G. A.; Salvador, P.; Dannenberg, J. J.; Dapprich, S.; Daniels, A. D.; Farkas, Ö.; Foresman, J. B.; Ortiz, J. V.; Cioslowski, J.; Fox, D. J. *Gaussian 09*, Revision B.01; Gaussian, Inc.: Wallingford, CT, 2009.

[45] Zhao, Y.; Truhlar, D. *Theor. Chem. Acc.* **2008,** *120*, 215-241.

[46] Scalmani, G.; Frisch, M. J. *J. Chem. Phys.* **2010,** *132*, 114110.

[47] Grimme, S.; Ehrlich, S.; Goerigk, L. *J. Comput. Chem.* **2011,** *32*, 1456-1465.

[48] Throughout the rest of the text, the mention of Ir-N bonding and the reactivity involving the Ir-N bond always refers to the Ir-N_{amido}, unless otherwise noted. The Ir-$N_{quinoline}$ bond is present in all the calculated complexes and without changes in connectivity at $N_{quinoline.}$

[49] Gregor, L. C.; Chen, C.-H.; Fafard, C. M.; Fan, L.; Guo, C.; Foxman, B. M.; Gusev, D. G.; Ozerov, O. V. *Dalton Trans*. **2010**, *39*, 3195-3202.

[50] DeMott, J. C.; Bhuvanesh, N.; Ozerov, O. V. *Chem. Sci*. **2013**, *4*, 642-649.

[51] Pandey, K. K. *Coord. Chem. Rev*. **2009**, *253*, 37– 55.

[52] Hebden, T. J.; Denney, M. C.; Pons, V.; Piccoli, P. M. B.; Koetzle, T. F.; Schultz, A. J.; Kaminsky, W.; Goldberg, K. I.; Heinekey, D. M. *J. Am. Chem. Soc.* **2008**, *130*, 10812-10820.

[53] Alcaraz, G.; Grellier, M.; Sabo-Etienne, S. *Acc. Chem. Res*. **2009**, *42*, 1640-1649.

[54] Plata, R. E.; Singleton, D. A. *J. Am. Chem. Soc*. **2015**, *137*, 3811-3826.

[55] There are multiple isomers of complex **11a** and they will be discussed in the context of Part VIII. The isomer **11a** is most pertinent to the analysis of Part II.

[56] We have also calculated the relative energy of TS1-8 vs compound 1 using different functionals. See Table S2 in the SI for details.

[57] **TS1-8** lies slightly higher in energy than **TS11a-12**, however, **TS1-8** does not need to be scaled throughout the continuous catalytic turnover via Parts II and III.

[58] See the SI for details.

[59] Crabtree, R. H. *Chem. Rev*. **2016**, *116*, 8750-8769.

[60] Kubas, G. J. *Proc. Natl. Acad. Sci. U.S.A*. **2007**, *104*, 6901-6907.

For Table of Contents Only

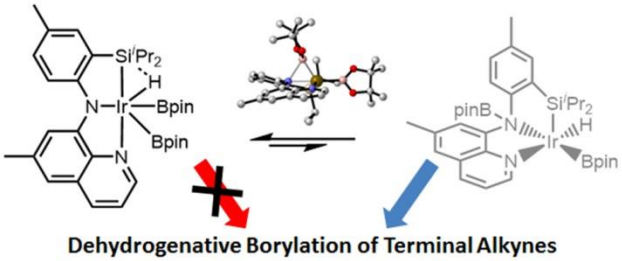

Dehydrogenative Borylation of Terminal Alkynes